Proceedings of ASME Turbo Expo 2020
Turbomachinery Technical Conference and Exposition
GT2020
September 21-25, 2020, Virtual, Online

GT2020-16151

A NEW TEST FACILITY FOR INVESTIGATING THERMAL BEHAVIOUR OF EFFUSION COOLING TEST PLATES FOR RQL COMBUSTORS

A. Picchi, A. Andreini, R.Becchi, B. Facchini
DIEF - Department of Industrial Engineering of Florence
University of Florence
Via S. Marta 3, 50139, Florence, Italy
antonio.andreini@htc.unifi.it

ABSTRACT

In aero engines the combustors are subjected to critical thermal conditions in terms of high temperatures and corrosive environment, which could affect the service life of the entire system. As well known, Thermal Barrier Coatings (TBC) and above all cooling systems represents the state-of-the-art in the nowadays protecting methods: the maximization of this beneficial effect is achieved by defining an optimal cooling arrangement and developing suitable manufacturing technologies for these systems. In modern aero-engine combustors, one of the most effective cooling scheme for liners is composed by an effusion perforation coupled with a slot system to start the film cooling. The cooling performances are deeply influenced by the mutual interactions between swirling and cooling flows. In addition, for typical Rich-Quench-Lean (RQL) combustor architectures, the injection of air provided to promoting the local break-down of the flame mixture fraction, deeply interacts with the swirled flow, generating recirculating structures capable of affecting the development of film cooling and making the design of cooling systems very challenging.

A new test facility for testing effusion test plates for RQL combustors applications has been developed with the final aim of comparing different cooling strategies and at the same time to collect data for numerical model validation. The experimental set-up consists of a non-reactive planar sector rigs with 5 engine-scale swirlers fed with air up to 250 $^{\circ}C$ *and* 3 *bar. The rig was equipped with outer/inner dilution ports, and a simple inner liner cooling scheme composed of effusion and a slot system: all these features, fed with air at ambient temperature, can be independently controlled in terms of mass flow.*

Using dedicated optical accesses, InfraRed (IR) camera tests were performed to retrieve overall effectiveness data imposing a temperature difference between swirling and cooling flows. To better understand those results, Pressure Sensitive Paint (PSP) technique was used to obtain reliable film effectiveness data decoupling the contribution of slot and effusion flows. The thermal characterization was supported by Particle Image Velocimetry (PIV) investigations on the median plane. Tests were performed at different pressure drops across swirler and varying the mass flows of slot and inner/outer liners. The analysis of the data highlighted the influences of the swirling flow on the overall thermal performance and the behaviour of the film cooling system.

NOMENCLATURE

Symbols

Bi	Biot Number	$[-]$
C	Mass fraction	$[-]$
DR	Density Ratio	$[-]$
d	hole diameter	$[m]$
HTC	Heat transfer Coefficient	$[W/m^2K]$
I	Momentum flux ratio	$[-]$
k	Thermal conductivity	$[W/mK]$
M	Molar mass	$[kg/kmol]$
m_{ratio}	Mass flow ratio	$-$
P	Static pressure	$[Pa]$
Re	Reynolds number	$[-]$
S	Hole Pitch	$[m]$
Stk	Stokes number	$[m]$
T	Temperature	$[K]$
V	Velocity	$[m/s]$
x	Axial coordinate	$[m]$
y	Radial coordinate	$[m]$

Greeks

η_{ad}	Film cooling adiabatic effectiveness	$[-]$
η_{ov}	Overall Effectiveness	$[-]$
μ	Dynamic Viscosity	$[Pa\ s]$

Subscripts

aw	Adiabatic wall
$cool$	Cooling flow
dil	Dilution
eff	Effusion cooling
eng	Engine Condition
ext	External flow
int	Internal hole flow
$main$	Mainstream flow
$no\ eff$	No effusion injection
ref	Reference
O_2	Oxygen
sw	Swirling Flow
w	Wall

Acronyms

CCD	Charged Coupled Device
CRZ	Central Recirculation Zone
CHT	Conjugate Heat Transfer
PIV	Particle Image Velocimetry
PSP	Pressure Sensitive Paint
RQL	Rich Quench Lean
UHC	Unburned Hydro-Carbons

INTRODUCTION

In the constant research of improved efficiency, modern aero-engine development pushes to continuously raise turbine inlet temperatures, resulting in severe conditions for combustion chamber liners. Combustor wall thermal safety is entrusted to high performance cooling systems, such effusion perforations, which have to deal with a mutual interactions with the swirling main flow.

The study of near-wall flows constitutes one of the most important topic in the engineering development of gas turbine combustors; with particular reference to the liners, such aspect is not only related to cooling and film protection, but it strongly deals with the local behaviour of the flame. The injection of air near to the wall,in fact, is well known to be responsible for the production of Unburned Hydro-Carbons (UHCs), caused by a local quench of the combustion process imputable to the leaning of mixture and/or a premature chilling of reacting gases [1]. Another consideration is the one related to the development of favourable situations for flame anchoring: high turbulence levels and low velocities are conditions that contextually occurs in near-wall regions, where the interaction between fluid structures can be responsible for the generation of shear layers and recirculating zones.

It is clear that correlative cooling efficiency approaches derived from laboratory tests with uniform inlet flow are not fully representative of such disturbed conditions. This leads to predictions that could be inconsistent with the realistic applications and that is why a thorough verification makes possible to assess such conditions, thus adjusting the design in agreement with the targets. In recent years, studies on the interaction between swirling structures and the film coverage layers are a topic of growing interest in literature.

An exhaustive study was performed by Patil et al. [2, 3] on both can and annular combustor simulators with the objective of numerically and experimentally investigating the effects of a swirling flow on the convective heat transfer in scaled up conditions. Tests were conducted without involving chemical reactions and with uncooled liners. The impingement on the liner surface of the highly energetic swirler shear layer leads to a substantial enhancement of the heat transfer coefficient with an augmentation value with respect to a fully developed pipe flow of about 6. Thus imply a severe impact on the performance of the liner cooling system and attest the importance of investigations under realistic swirling conditions.

This aspect was fully remarked by the thorough experimental analysis conducted by Wurm et al. [4, 5] and by Andreini et al. [6, 7, 8]. Both research groups carried out several measurement campaigns on atmospheric enlarged-scale rigs, replicating three sectors of a combustion chamber in a planar arrangement. Impact of the mainstream swirling flow on different effusion cooling patterns was analysed varying geometric parameters and operating conditions by means of flow field investigations and liner thermal characterizations. Outputs confirm the presence of critical regions for the liner with coolant protection significantly weaken by the main flow action.

A further step towards realistic engine conditions repro-

duction was added by Shanghai Jiao-Tong University research group [9, 10], which performed experiments involving reacting processes in order to take account of the flame pattern and combustion heat release. A scaled three sector annular combustor with effusion cooling plates equipped on both outer and inner liners was employed to perform an IR thermography for wall temperature field measurement.
PIV and IR termography caractherization of an engine scale single-can combustors was recently conducted at Virginia Tech Advanced Power and Propulsion Laboratory [11, 12]. These investigations have addressed the impact of important combustor parameters on the reacting fluid dynamics.

Starting from these demands, present study reports the development of a new RQL combustor simulator aimed to perform test on 1:1 engine scale components under relevant operating conditions. Rig is opportunely designed to allow the employment of Particle Image Velocimetry for flow field investigation and the use of IR thermography and PSP technique for inner liner thermal characterization.

EXPERIMENTAL APPARATUS

The new experimental apparatus consist of a linear, non-reactive, five injectors combustion chamber simulator operating at warm conditions. The model reproduces in $1:1$ engine scale five sectors of a typical RQL combustor architecture and thanks to the multiple-injectors configuration adopted allows to recreate periodicity conditions in the central swirler region. The design of the rig was strongly affected by the requirements of planned measurement campaigns, demanding for several optical accesses to the test section and for flexibility of investigating different liner cooling geometries.

A cross-sectional sketch of the apparatus, with a zoomed view of the test section, is reported in Fig. 1. The five injectors are fixed at the dome in a linear arrangement. Since non-reacting processes are involved in the present study, the fuel lines are not present and the respective housings are opportunely plugged in order to accurately reproduce the real swirling behaviour.

The measurement target is represented by the inner liner, which is positioned in the bottom side of the test section, above a large plenum equipped with a grid to ensure an uniform coolant feeding. The liner is composed of three removable metal coupons, the two lateral plates present only quenching holes, while the central one, which is the objective of the investigation, can be equipped with different effusion cooling geometries. Furthermore, a starter slot system composed of discrete holes, is present at inner liner-dome interface to generate film cooling in the initial part of the plate.

In this preliminary experimental campaign a coupon with a pattern of inclined cylindrical holes. The effusion geometry presents a constant hole pitch to diameter ratio, equal to $S/d = 12$, in both streamwise and spanwise direction, and a length to diameter ratio l/d equal to 6. The distance between the slot exit plane and the first row of holes is about $18 \cdot d$. The plates is manufactured using metal addictive technologies with effusion holes realized by means of laser drilling process.

In order to guarantee a realistic flow field inside the test section, also the outer liner is equipped with quenching holes. In terms of passage areas, four quenching holes, both for inner and outer liner, are present in a single combustor sector. Quenching holes diameter is about 9 times the effusion holes diameter.

A total of three optical accesses are present in the test rig in order to perform PIV, Infrared thermography and PSP technique. Two borosilicate glass windows are used during flow field investigation: one in the outlet side of the test rig to guarantee the introduction of the laser sheet and one on the lateral side of the test section to allow the camera acquisition. For investigations devoted to estimate the cooling efficiency of the inner liner a transparent window is installed on the top side of the test section, nature of this element is subjected to change according to the rig operating conditions.

As schematized in Fig. 2, the test rig is integrated in a dedicated hot wind tunnel with compressed air delivered by two

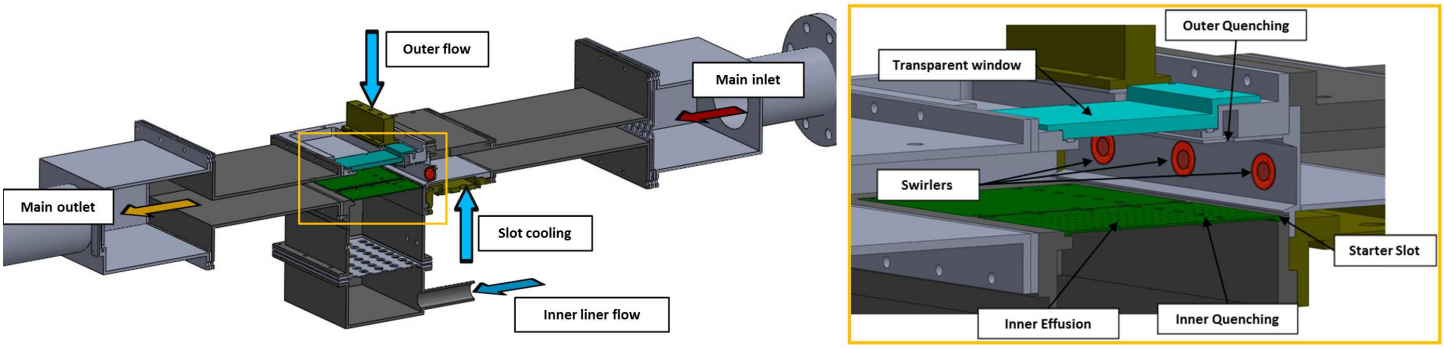

FIGURE 1: Cross sectional view of the test rig with a detailed section of the test section

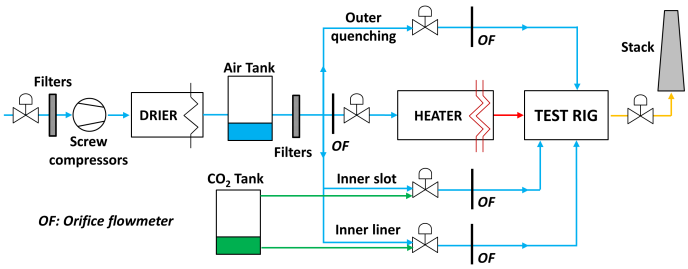

FIGURE 2: Schematic diagram of the test facility

screw compressors accounting for a maximum total mass flow rate of about 1 kg/s at a maximum pressure of 10 bar. Before entering within the facility air passes through a drier (dew point $-20\ ^{\circ}C$) , which lowers the mass flow temperature and removes the humidity. A 2 m^3 tank is then inserted along the line in order to dump pressure fluctuations and a set of filters have the task to eliminate potential impurities from the flow. Part of the air, representing the mainstream flow devoted to feed the set of swirlers, is sent to a 600 kW electric heater, which allows to increase the compressed air temperature up to a maximum limit of 520 K, that represent the maximum limit arranged for the current experimental campaign. Three additional feeding lines with air at ambient temperature are employed to deliver the coolant to combustion chamber quenching holes and to the inner liner (effusion and starter slot), for these last cooling features is possible also to deliver technical gases, as carbon dioxide, in order to perform PSP tests. All the four lines are equipped with dedicated calibrated orifice flowmeters and regulating valves, allowing the separate control of each stream.

In order to regulate the pressure levels inside the test section and to set the desired conditions, a counter-pressure valve is inserted between the test rig outlet duct and the piping system that carry the air to the stack.

Alongside the entire test rig are installed several thermocouples and static pressure taps in order to monitor and control the operating conditions. Temperature measurements are acquired by a data acquisition/switch unit HP/Agilent 34972A, with external reference junction. A total of seven K-type thermocouples ($\pm 1\ K$ uncertainty) are employed to measure the air temperature upstream and downstream the dome and inside the coolant feeding plenums. During InfraRed thermography test, six supplementary thermocouples, embedded on the effusion coupon, are acquired to evaluate liner metal temperature. A pressure scanner NetScanner System 9116 with temperature compensated piezo-resistive relative pressure sensors (maximum uncertainty $\pm 52\ Pa$ with a level of confidence of approximately 95%) is used to measure static pressure in different locations inside the rig. Mainstream, inner liner, outer quenching and starter slot mass flow rates are measured by means of calibrated orifices (according to the EN ISO 5167-1 standard); the maximum uncertainty for mass flow rate measurement is about 4%. During tests, an in-house developed Labview software tool monitors continuously all the parameters and permits to record test points when the stationary conditions are reached.

DIMENSIONAL ANALYSIS

The final aim of the rig is to provide reliable measurements of thermal performance of different cooling system arrangements for liners based on effusion perforations. The system thermal characteristic will be quantified by means of two parameters: overall effectiveness which represents the scaled temperature of the liner and hence it includes the effect of convective loads and film protection, and adiabatic effectiveness commonly used to define the film cooling capabilities (i.e. adiabatic wall temperature distributions).

Since the tests are performed at laboratory conditions, the scalability of those quantities to the engine cannot be performed directly. Overall effectiveness tests are set-up without the effect of combustion and simulating the temperature difference between hot gases and coolant preheating the mainstream at around $250\ ^{\circ}C$. However, if the typical non dimensional parameters of engine affecting the heat transfer phenomena are respected and a representative swirling flow is reproduced the experiments can provide a valid support to the combustors design. Beyond the possibility of performing a delta-based comparison between geometries and to provide a database for CHT simulations, the test rig can highlight critical regions and underline the behaviour of film cooling.

In the open literatures, several authors have discussed the role of the main non dimensional parameters on the final overall effectiveness distribution especially for test arrangement with uniform main flow typically of turbine airfoil experiments ([13, 14, 15]). All these works agree with the importance of replicating:

- the adiabatic effectiveness (i.e the film cooling behaviour);
- the heat transfer ratio (HTC_{ratio}) between coolant and mainflow side which balance the external heat load and the internal heat removal;
- the Biot number in order to replicate the temperature gradients inside the component.

In particular the Biot number, as discussed by Martiny et al. [16], has a strong influence on overall distribution in effusion test cases. In laboratory condition, several researchers have conditioned the value of Biot number selecting a different material for the test plate or acting on the scale dimensions [17]. The recent interest of scientific research on heat transfer is moving toward additive manufacturing components at 1:1 scale in order to take into account effects of additive manufacturing [18]. For this reason the scale 1:1 and the use of engine materials become

constrains of the test rig design, limiting the possibility of perfectly match the non dimensional parameters cited above.

Starting from these constraints, and having in mind the necessity of replicating a representative swirling flow the test rig has been designed to work at engine swirl Reynolds number. The Reynolds similitude is not a mandatory conditions for overall effectiveness distribution tests, nevertheless it should be respected especially for combustion chamber working at moderate Reynolds value in order to correctly replicate the development of main flow in the chamber and, in some cases, the swirler behaviour (Gomez-Ramirez et al. [11]). As a consequence of imposing a Re_{sw} value, the swirler behaviour can be controlled by increasing the pressure of the rig in order to replicate or limit the chamber pressure drop to typical engine values.

Regarding the main flow, in a RQL combustor the mass flow adducted in the test chamber from dilution ports plays a key role. As a first choice the mass flow ratio between swirling flow and dilution flow should be replicated. Since the dilution ports are fed with the same plenum of the effusion chamber, this assumption allows to replicate directly the coolant consumption which is one of the most important parameter for film effectiveness [19]. Another relevant parameter for film cooling is the density ratio: in the present facility the DR was set around 1.7, it is obtained increasing the temperature of the swirl flow up to around $250°C$ and keeping the coolant at ambient temperature. Despite this value is not high enough to represent typical values of the engine its influence on effusion cylindrical holes is less important respect to the BR (i.e. coolant consumption) when, as in the present test case, the perforation works in fully penetration regime [19].

As a consequence of setting swirler mass flow (Re_{sw}), pressure ($Mach$ number), coolant flow (BR) and flows temperature, the other relevant parameters affecting wall temperature are frozen. In particular the Reynolds of the coolant is not perfectly matched since it depends directly on the ratio of viscosity between engine and rig. Moreover the ratio between external and internal HTC (heat sink effect) depends directly from the ratio of viscosity and thermal conductivity. Assuming approximately a direct relation between Nusselt number and $Re^{0.8}$, the deviation of HTC ratio can be quantified as:

$$\left(\frac{HTC_{ext}}{HTC_{int}}\right)_{engine} \Big/ \left(\frac{HTC_{ext}}{HTC_{int}}\right)_{rig} \approx \approx \left(\frac{k_{main}\mu_{cool}^{0.8}}{k_{cool}\mu_{main}^{0.8}}\right)_{engine} \Big/ \left(\frac{k_{main}\mu_{cool}^{0.8}}{k_{cool}\mu_{main}^{0.8}}\right)_{rig} \quad (1)$$

Finally, the Biot number is strictly dependent on the value of thermal conductivity and hence on the expected liner temperature. At engine condition the thermal conductivity of the liner wall is more than twice the value assumed at rig temperature: this behaviour helps to compensate the variation of flow thermal conductivity between rig and engine which in turns affects the HTC through the Nusselt number definition.

TABLE 1: Deviation of similitude parameters respect to engine reference condition at nominal test point (TP1)

Re_{sw}	Re_{cool}	mass flow ratio	DR	Bi	HTC_{ratio}
0%	-13%	0%	-32%	-4%	-20%

To summarize, in the Table 1 the deviation of the typical non dimensional parameters at nominal test point respect to the engine are reported: the values are fairly in line with the reference values and the maximum deviation is due to the DR.

To complete the characterization of the liner thermal performance specific film effectiveness tests are required. For the capability of retrieving high resolution results the PSP technique is selected; due to the paint formulation the technique requires to define a cold test point at ambient pressure. As a consequence, if the chamber pressure drop and mass flow ratio are preserved, the PSP test condition exhibits lower Reynolds while the DR is almost equal to the warm conditions thanks to the use of carbon dioxide as a tracer ($DR = 1.5$). Specific tests are conducted varying the swirler mass flow (Re number) and keeping constant the mass flow ratio to asses the impact of Reynolds number on the near wall mixing phenomena; as illustrated in Fig. 3 the impact of the working Re on the film effectiveness profiles along the liner is almost negligible giving the possibility to compare warm and cold test points.

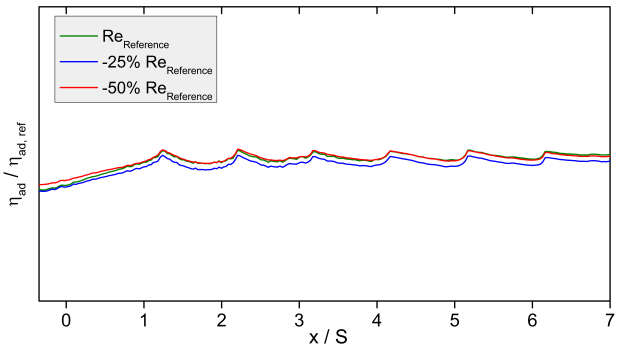

FIGURE 3: Laterally average adiabatic effectiveness distributions: impact of Reynolds number on film cooling

MEASUREMENT TECHNIQUES

The test rig has been expressly designed to guarantee the execution of several experimental investigations on different liner cooling systems. Estimation of overall effectiveness and film cooling adiabatic effectiveness distributions are respectively

achieved through the exploitation of Infra Red thermography and PSP technique. Furthermore, to support these analysis, the apparatus allows the opportunity of performing average PIV measurements on the rig median plane.

Flow field characterization

The first stage in analysing the combustor consisted in evaluating the internal aerodynamics, with the aim of understanding the flow interactions between the central swirler and quenching holes jet. A standard 2D PIV technique has been chosen for carrying out average flow field measurements on the rig median plane.

In Fig. 4 is reported the measurement setup for the test rig to perform the investigation. Tests are carried out employing a Dantec Dynamic 2D PIV system, consisting of a 120 mJ New Wave Solo Nd:YAG pulsed laser operating with a wavelength of 532 nm and a Phantom Miro 320S camera, operating at a data rate of 15 Hz, for images acquisition. The laser sheet is created by the optics embedded in the New Wave Solo Nd:YAG system, consisting in a cylindrical lens that expands the laser into a plane and a spherical one that compresses the plane into a thin sheet (thickness always below 1 mm). The introduction of the laser sheet inside the test section is provided by means of a 45 deg mirror, through the borosilicate glass windows positioned in the rear side of the rig.

The optical access for camera acquisition is guaranteed by an other borosilicate glass window located on the lateral side of the test section. The seeding particles are generated by a Laskin nozzle and consist of silicone oil droplets of proper dimension and density ($Stk < 1$). For the mainstream flow, the injection takes place by means of a drilled pipe installed in the inlet plenum, while, for the inner liner, through a pipe connected directly to the coolant plenum.

The control of the system and data post-processing operations are performed with the commercial software Dantec DynamicStudio 4.0. For each test point, about 500 image pairs are acquired with a time delay of 8 μs. Scale factor has been limited to about 7 in order to achieve a suitable image resolution for subpixel interpolation. For images post-processing, an iterative approach based on adaptive cross-correlation algorithm is employed and the resulting average velocity field is then subjected to a peak-height validation. Uncertainty evaluation is carried out using the approach developed by Charonko and Vlachos [20], consisting in correlating the uncertainty bounds to the cross-correlation peak ratio; this approach leads to uncertainties low as about 3% in the areas with the highest measured velocities and up to 17% in low-velocity and recirculation zones.

Due to light reflections and rig optical access constraints, the minimum distance from the chamber walls covered by the investigation is about 1.5 mm.

Overall effectiveness measurement

For liner thermal investigations an Infrared thermography is employed with the aim to obtain high resolution temperature distributions on the central region of the test article. The IR camera used in this activity is a FLIR SC6700, working in the medium wavelength range ($\lambda = 3-5\ \mu m$) and able to provide thermal images with a spatial resolution of 640x512. The camera incorporates a cooled Indium Antimonide (InSb) detector with a 15 μm pixel-pitch. In order to cover the entire temperature span, the camera operates employing four active pre-set operating modes, providing adjustable integration times.

The optical access to the effusion coupon is guaranteed by installing a Sapphire window within a dedicated housing on the top side of the chamber Fig. 5. Internal surfaces of the chamber and the effusion coupon are sprayed with an opaque black high temperature paint to avoid reflections and to enhance the emissivity of the coupon. In order to correctly adjust the raw signal values of the IR detector, the in-situ calibration approach proposed by Martiny et al. [21] is employed. For this reason, on the effusion coupon are incorporated six thermocouples. Implementation of this fitting procedure has led to an average error of about 5% with respect to thermocouples reading values. Surface temperature distributions on the plate (T_w) is then used to estimate overall cooling effectiveness:

$$\eta_{ov} = \frac{T_{main} - T_w}{T_{main} - T_{cool}} \tag{2}$$

where T_{main} represents the mainstream temperature, evaluated upstream the set of swirlers and T_{cool} the coolant temperature measured inside the feeding plenum positioned underneath the liner.

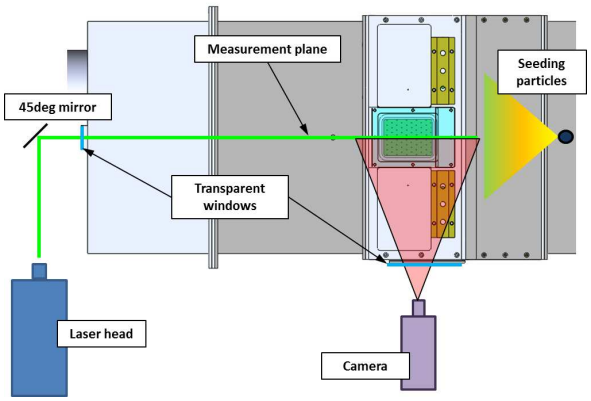

FIGURE 4: Schematic PIV test rig setup

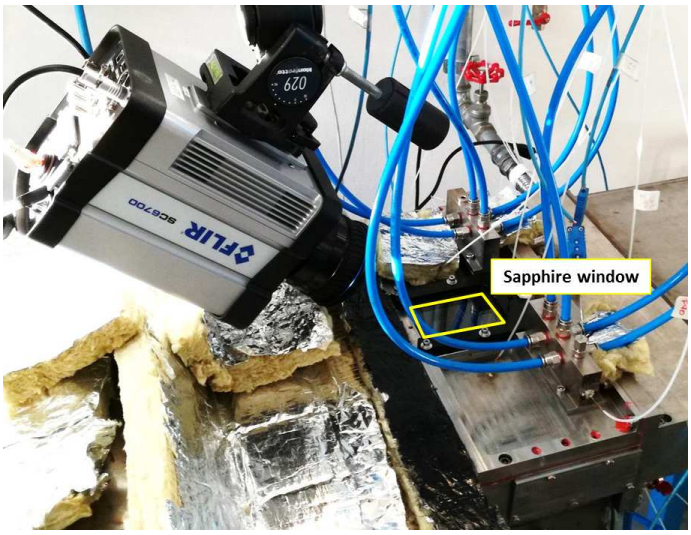

FIGURE 5: Test rig view during Infra-Red thermography campaign

Adiabatic film cooling effectiveness investigation

To examine the liner behaviour in terms of film covering a Pressure Sensitive Paint technique is employed to achieve bi-dimensional distributions of adiabatic effectiveness. PSP are organic substance composed of oxygen-sensitive molecules embedded in a polymeric binder. Thanks to the luminescence behaviour of these molecules is possible to detect oxygen partial pressure in the surroundings of the painted wall, which in turns, can be linked to local oxygen concentrations. Using as coolant a tracer gas without free oxygen and considering valid the temperature and mass transfer analogy, the definition of adiabatic film cooling effectiveness can so be formulated as reported below:

$$\eta_{ad} = \frac{T_{main} - T_{aw}}{T_{main} - T_{cool}} \equiv \frac{C_{main} - C_w}{C_{main}} = \\ = 1 - \frac{1}{\left(1 + \left(\frac{P_{O_2;main}/P_{O_2;ref}}{P_{O_2;cool}/P_{O_2;ref}} - 1\right)\frac{M_{cool}}{M_{main}}\right)} \tag{3}$$

where T_{aw} is the adiabatic wall temperature and C_{main} and C_w are respectively the oxygen concentration in the main flow and in proximity of the painted surface. More details on PSP technique and the adopted procedure can be found in [22]. PSP employed in the present activity is an UniFIB formulation supplied by Innovative Scientific Solutions Inc. The correct excitation to the target surface is provided by an high performance UV LED Illuminator system IL104 and image acquisition is carried out exploiting a 1600x1200 resolution 14-bit CCD camera (PCO.1600) equipped with a 610 *nm* red filter. Carbon dioxide is used as foreign gas, for this reason during this campaign the inner slot and inner liner feeding lines are switched through a system of control valves from the compressed air line to a CO_2 pressure tank. Since PSP tests are conducted at nearly atmospheric conditions a PMMA windows is used as optical access on the top side of the test section.

TABLE 2: Test Matrix

	Re_{sw}	m_{ratio}	I	DR
TP1		$m_{ratio,eng}$	$+40\%I_{eng}$	
TP2	$Re_{sw,eng}$	$-20\%m_{ratio,eng}$	I_{eng}	1.7
TP3		$-40\%m_{ratio,eng}$	$-40\%I_{eng}$	

TEST MATRIX

According to the criteria reported in the dimensional analysis a nominal reference test point (TP1) has been specified for the tests, it was defined starting from the definition of coolant consumption (m_{ratio}) and momentum flux ratio (I):

$$m_{ratio} = \frac{m_{dil}}{m_{sw}}; \quad I = \frac{m_{ratio}^2}{DR} \tag{4}$$

Additional test points are explored during the experiments in order to asses the effect of different levels of coolant consumption, and also including/excluding the effect of the starter film cooling. In case of test points with slot injection, the slot is fed with the same pressure drop of the inner liner. The InfraRed camera experiments are performed heating up the swirlers air up to $520K$ keeping the coolant lines at room temperature.

A summary of the test points reported in the present paper have been listed in Table 2. The DR value reported in the Test Matrix refers to the overall effectiveness tests, as already mentioned for the PSP measurements the DR is around 1.5 (CO_2 foreign gas) and the temperature of the mainstream is nearly ambient. It is worth to notice that TP2 and TP3 operating conditions are defined reducing progressively the coolant through inner and outer liners, in particular TP2 is set in order to match the dilution momentum flux ratio of engine.

RESULTS

Flow Field Characteristics

Liner thermal behaviour and hence cooling system performance are strongly affected by general flow field established in the combustion chamber. For a deeper understanding of

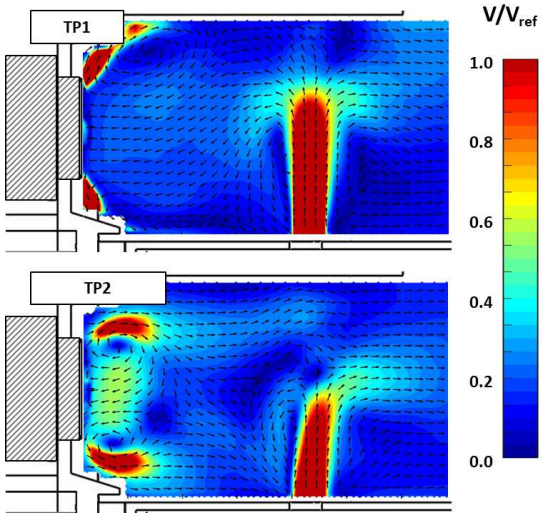

FIGURE 6: Average velocity maps (TP1 and TP2 conditions)

test rig aerodynamic characteristics a dedicated PIV campaign was performed. In Fig. 6 are reported the average flow field maps measured on the median plane for two of three test points investigated; 2D distributions show the magnitude of the PIV velocity normalized by a reference value.

For the reference test point (TP1), typical main flow structures of swirl stabilized flames are highlighted, the jet exiting from the swirler is spread by the large central recirculation zone induced by the vortex breakdown onset. Flow field estimation near the dome is affected by critical reflections issues that tends to reduce the actual velocity magnitude, this effect seems to be more intense on the lower side of the swirler leading to a strong jet asymmetry. Quenching hole jet presents a significant penetration in the main flow preserving a coherent flow structure beyond the swirler axis, a substantial amount of air from the quenching flow tends to be summoned by the CRZ, contributing to widen the swirling jet expansion.

Reducing the inner liner mass flow rate for matching engine momentum flux ratio (TP2), a drastic change in swirler behaviour, and hence in chamber flow field, is observed. A limited swirler-quenching hole interaction leads to the development of a short and tight inner recirculation zone, with annular swirler jet characterized by a limited expansion which is confined by the slot overhang. Quenching hole jet is consistently less intense and is deviated downstream from its outlet axis. In the upper side of the test section, the absence of dilution flow structure in the center plane permits at the swirler jet stream to conduct to strong positive axial components near the liner. Reducing again the coolant mass flow towards the TP3 the flow structures remain similar the ones described for the TP2.

Since these two types of swirler behaviour will have a strong impact on the liner thermal performance a specific investigation has been conducted. In particular several test points has been acquired reducing progressively the coolant mass flow (from TP1 condition towards TP3). Moreover additional acquisitions were performed setting different values of Re_{sw} and DR by reducing the preheating of mainflow. The main outcome coming from this extensive analysis is a sudden change from the flow structure with a wide opening angle of the swirling jet (regime A), as described for TP1, to the more confined swirling region along the centerline recognized in TP2 (regime B). The sudden transition of the swirler behaviour underlines unstable interactions phenomena between swirled and dilution ports flows in the primary zone upstream the dilution holes and the onset of the two regime comes directly from the dilution and swirling flow interactions.

Despite the analysis and the regime transition should be considered strictly valid for the present configuration (swirler, effusion porosity and dilution ports positions), it allows to underline an interesting unstable behaviour which in principle could affect other burners operating in RQL architectures. As will be discussed in the further sections, one of the main drawback of the two regime onset is a complete different liner thermal behaviour.

Overall Effectiveness Maps

Moving the focus to liner thermal investigation by means of IR thermography, in Fig. 7 are showed overall effectiveness distributions obtained for two operating conditions. The central masked out region of the maps represents the dilution zone location. For TP1, in the initial part of the liner is possible to recognize a low effectiveness region identifying the stagnation zone of the swirling jet impinging the liner. Due to the wide expansion of the swirling flow (regime A), jet impingement occurs very close to the combustor dome. It's interesting to note that the slight asymmetry of this high temperature area is coherent with swirler rotating direction. Downstream the quenching ports, strong mixing phenomena have take place and film cooling superposition effect became significant, leading to higher overall effectiveness values. Maximum η_{ov} value is detected in correspondence of the last row of holes investigated at a radial location of $y/S = 1.5$

A substantially different 2D distributions are observed for TP3, while, as a general result, reduced coolant mass flow rate evidently leads to a liner temperature enhancement. According to previous flow field investigation and relative identified regime B, the reduced swirling jet expansion drastically changes the shape of the impinging region. The high temperature zone shows an approximately symmetric distribution across the median plane and seems to protract downstream the quenching holes, taking advantage of their limited jet momentum.

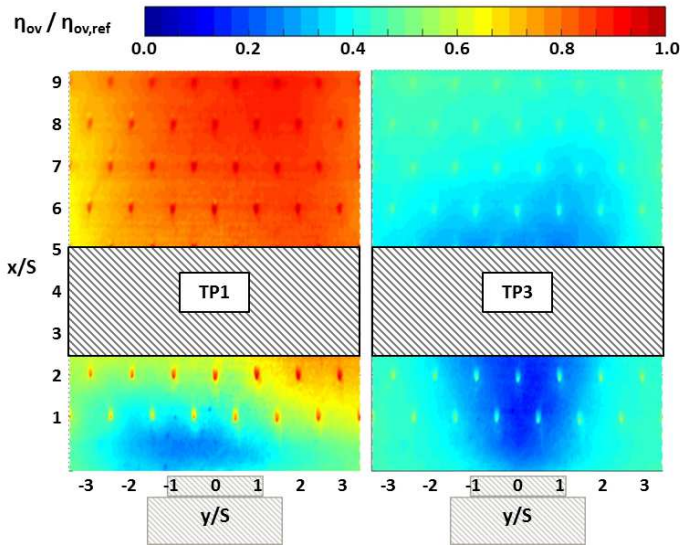

FIGURE 7: Normalized overall effectiveness maps. TP1 and TP3 results comparison

Adiabatic Film Cooling Effectiveness Results

To conclude the analysis, results from adiabatic film cooling effectiveness campaign are hence reported. Due to the nature of the measurement and test rig geometry, the whole inner liner is fed with technical gas, thus implicates a false contribution to liner cooling supplied by the quenching holes, which doesn't allow to directly and selectively estimate the effusion system performance. Nevertheless results can provide substantial information on the mixing phenomena between the different coolant flows and allow to properly compare different effusion cooling patterns.

Normalized η_{ad} maps displayed in Fig. 8, for two test points with no slot injection, highlight a coherent behaviour with respect of overall effectiveness measurement. TP1 shows a quite uniform protection downstream the first row of holes; in the central region of the plate the coolant injection produces short traces due to the interaction of the swirling flow, while for $y/S < -1.5$ and $y/S > 1.5$ more coherent and axially directed traces are observed. TP3 distribution highlights a more intense decay in film protection close to the central quenching hole with coolant traces directions which seem to be deeply affected by the general chamber flow field.

A more quantitative comparison is reported in Fig. 9 by means of normalized η_{ad} laterally averaged trends. The plots allow to underline the effect of the slot system. For TP1 the slot impact is appreciable until the first row of effusion holes, going beyond the quenching jets action seems to weaken the slot

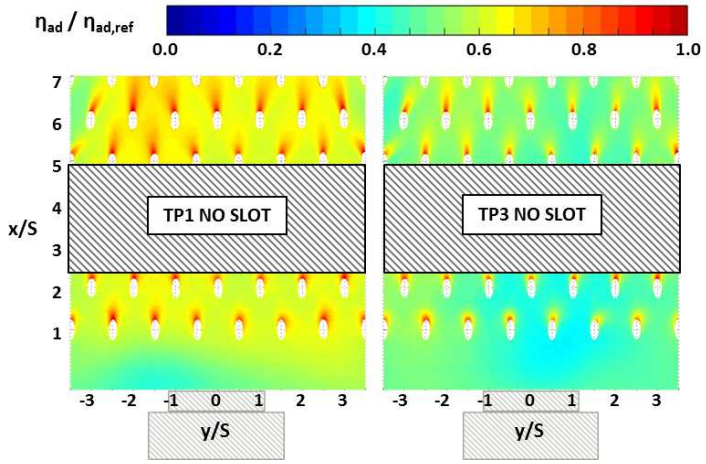

FIGURE 8: Normalized adiabatic effectiveness maps. TP1 (no slot) and TP3 (no slot) results comparison

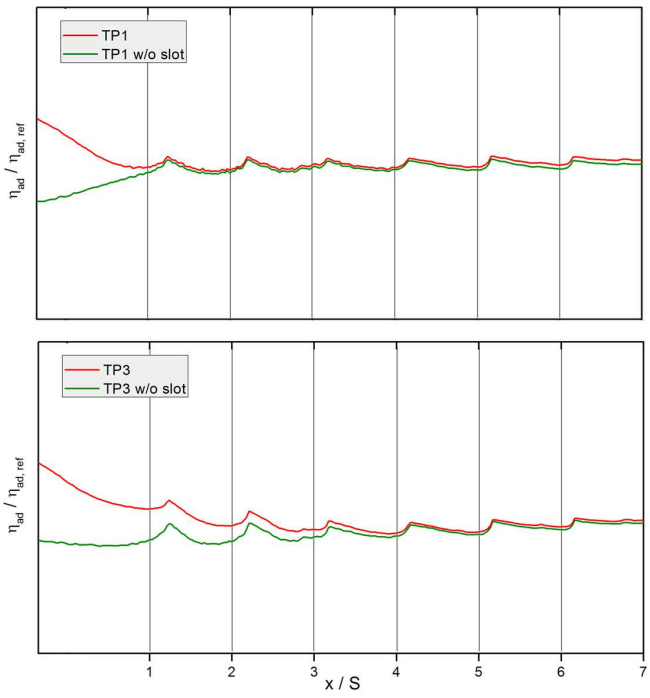

FIGURE 9: Laterally averaged adiabatic effectiveness distributions: slot cooling impact

structure leading to a very similar distribution with respect of reference condition. In the case of TP3, due to the reduced momentum of quenching jets and the less intense interaction with the swirling flow, slot coolant is able to remain attached to the wall for a more axially extended region of the liner.

As already discussed the film effectiveness maps come directly from the coolant concentration measurements near the wall generated by both effusion and dilution ports injection. As a consequence, one of the main drawback of this analysis, is the inability to distinguish in the results the contribution to the effectiveness coming from the film cooling perforation. One of the feasible way to decouple this contribution from the global effectiveness map is to apply a superposition approach derived directly from the theory of Sellers [23].

The basic idea is to perform a dedicated PSP test with effusion system plugged keeping only the dilution ports open ($\eta_{ad,noeff}$) and setting the flow parameters at the same value of the reference global effectiveness test. The outcome of this investigation will be a sort of effectiveness map which represents the dilution flow concentration near the liner. The presence of dilution flow near the wall is due to the intense mixing between dilution jets and swirling core region which generally occurs far from the wall. As a consequence, the concentration of dilution flow acquired with this dedicated test can be assumed as the reference concentration of coolant experienced above the film layer by the effusion system ($\eta_{ad,eff}$). Under this assumption the contribution of the effusion can be decoupled by the film effectiveness test (η_{ad}) with both effusion and dilution injection as:

$$\eta_{ad;eff} = \frac{\eta_{ad} - \eta_{ad;noeff}}{1 - \eta_{ad;noeff}} \tag{5}$$

Eq. 5 corrects the effectiveness maps especially in the region with lower effectiveness values while it preserves the area with higher effectiveness (i.e. if $\eta_{ad} = 1 \Rightarrow \eta_{ad;eff} = 1$)

It is worth to notice that the hypothesis used for this analysis could be weakened in presence of strong mixing between effusion film layer and swirling flow and when the effusion injection is able to influence the main flow structures. Nevertheless, the effectiveness maps assume an improved readability that helps,

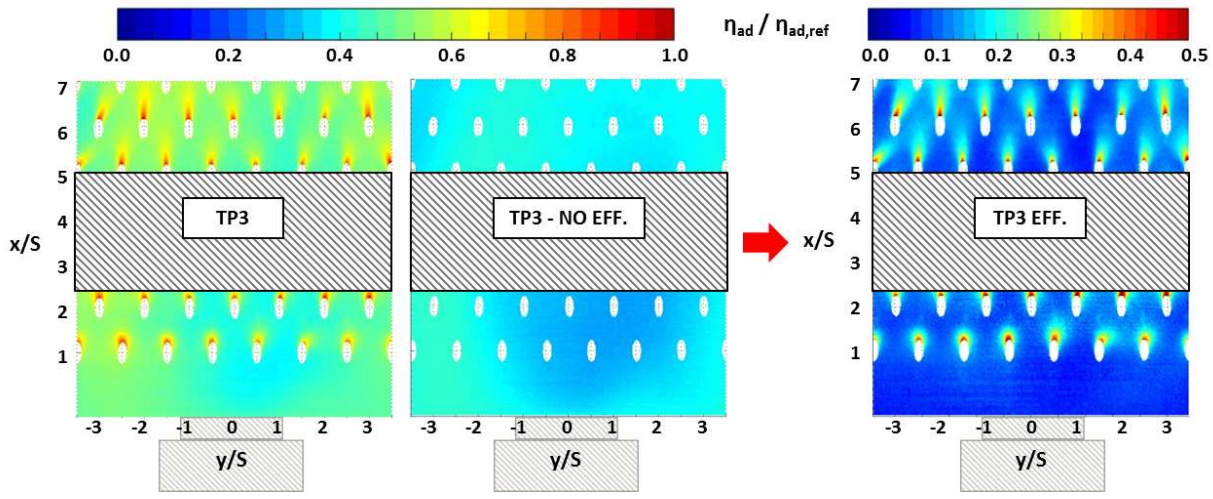

FIGURE 10: Adiabatic film effectivenss of effusion flow from decoupling approach

for example, to perform a more quantitative comparison between different plates with various perforation schemes or hole manufacturing technologies.

As an example of the proposed methodology, Fig. 10 reports the results for the TP3 test with no slot injection. The effusion film map clearly shows the short coolant traces which characterized the region upstream the dilution holes. In this area the traces are also spread in laterally direction due to the unsteadiness generated by the swirling flow. Downstream the dilution, the average level of film effectiveness is enhanced by the film superposition and the jet traces are more elongated. Upstream the first row of holes the average effectiveness level presents values above zero: this behaviour can be attributed to the recirculation of effusion flow in the corner region as already underlined in the open literature [8].

CONCLUSIONS

In this paper a new test facility for liner cooling system for RQL combustor has been presented and commissioned, testing a first liner configuration with effusion pattern composed by inclined cylindrical holes. The test rig is a linear penta-sector combustor simulator at real engine scale, equipped with dilution holes on outer and inner liners as typical of RQL architectures. The dimensional scale equal to the engine reference condition was imposed in order to realize the liner plate with the same manufacturing techniques used in the real hardware application.

The rig has been developed to perform the following analysis respecting approximatively the main non dimensional parameters:

- PIV investigation on median plane;
- overall effectiveness imposing a relevant temperature difference between swirling flow and coolant;
- adiabatic effectiveness using PSP technique.

The results on first effusion geometry show a strong impact of swirling flow on both temperature and film maps especially on the first part of the liner upstream the dilution ports at nominal test point. Reducing the flow from the dilution a sudden change of the swirling structure is recognized: it was demonstrated that such unstable phenomena linked to the interaction of dilutions and swirling flow in the primary region has a primary role in the liner temperature distribution which in turn influences the expected life of the hardware. Finally, a methodology based on superposition approach has been proposed to analyse the film effectiveness generated by effusion injection. The resulting effectiveness map, decoupling the contribution of dilution holes, clearly underlines the different behaviour of the jet upstream the dilution hole, with short traces due to the swirling flow interactions, respect to the downstream region with elongated traces and a better wall protection. Across all the investigated region, the coolant traces are characterized by an important lateral spreading coming from the jet unsteadiness prompted by the swirling flow.

The rig offers a valuable apparatus to compare different cooling technologies at relevant thermal test conditions; in addition further thermal analysis of the results could be exploited to retrieve the heat transfer coefficient on the liner cold side using FEM simulation of experiments.

ACKNOWLEDGMENT

The authors wish to gratefully acknowledge SOPRANO (SOot Processes and Radiation in Aeronautical inNOvative combustors) Consortium for the kind permission of publishing the results herein. This project has received funding from the European Union's Horizon 2020 research and innovation programme under Grant Agreement No. 690724.

References

[1] Mellor, A.M. *Design of modern turbine combustors*. (Combustion treatise). Academic Press, 1990. ISBN 9780124900554.

[2] Patil, S., Abraham, S., Tafti, D., Ekkad, S., Kim, Y., Dutta, P., Moon, H.-K., and Srinivasan, R. Experimental and numerical investigation of convective heat transfer in a gas turbine can combustor. *Journal of Turbomachinery*, 133(1):011028, 2011. doi: 10.1115/1.4001173.

[3] Patil, S., Sedalor, T., Tafti, D., Ekkad, S., Kim, Y., Dutta, P., Moon, H., and Srinivasan, R. Study of flow and convective heat transfer in a simulated scaled up low emission annular combustor. *Journal of Thermal Science and Engineering Applications*, 3(3): 031010, 2011. doi: 10.1115/1.4004531.

[4] Wurm, B., Schulz, A., and Bauer, H.J. A new test facility for investigating the interaction between swirl flow and wall cooling films in combustors. In *Proceedings of the ASME Turbo Expo*, 2009. doi: 10.1115/gt2009-59961.

[5] Wurm, B., Schulz, A., Bauer, H.J., and Gerendas, M. Impact of swirl flow on the cooling performance of an effusion cooled combustor liner. *Journal of Engineering for Gas Turbines and Power*, 134(12):121503, 2012. doi: 10.1115/1.4007332.

[6] Andreini, A., Facchini, B., Becchi, R., Picchi, A., and Turrini, F. Effect of slot injection and effusion array on the liner heat transfer coefficient of a scaled lean-burn combustor with representative swirling flow. *Journal of Engineering for Gas Turbines and Power*, 138(4):041501, 2015. doi: 10.1115/1.4031434.

[7] Andreini, A., Becchi, R., Facchini, B., Mazzei, L., Picchi, A., and Turrini, F. Adiabatic effectiveness and flow field measurements in a realistic effusion cooled lean burn combustor. *Journal of Engineering for Gas Turbines and Power*, 138(3):031506, 2015. doi: 10.1115/1.4031309.

[8] Andreini, A., Becchi, R., Facchini, B., Picchi, A., and Peschiulli, A. The effect of effusion holes inclination angle on the adiabatic film cooling effectiveness in a three-sector gas turbine combustor rig with a realistic swirling flow. *International Journal of Thermal Sciences*, 121:75–88, 2017. doi: 10.1016/j.ijthermalsci.2017.07.003.

[9] Ge, B., Ji, Y., Chi, Z., and Zang, S. Effusion cooling characteristics of a model combustor liner at non-reacting/reacting flow con-

ditions. *Applied Thermal Engineering*, 113:902–911, 2017. doi: 10.1016/j.applthermaleng.2016.11.049.

[10] Ji, Y., Ge, B., Chi, Z., and Zang, S. Overall cooling effectiveness of effusion cooled annular combustor liner at reacting flow conditions. *Applied Thermal Engineering*, 130:877–888, 2018. doi: 10.1016/j.applthermaleng.2017.11.074.

[11] Gomez-Ramirez, D., Kedukodi, S., Ekkad, S.V., Moon, H.-K.X., Kim, Y., and Srinivasan, R. Investigation of isothermal convective heat transfer in an optical combustor with a low-emissions swirl fuel nozzle. *Applied Thermal Engineering*, 114:65–76, 2017. doi: 10.1016/j.applthermaleng.2016.11.154.

[12] Park, S., Gomez-Ramirez, D., Gadiraju, S., Kedukodi, S., Ekkad, S.V., Moon, H.K., Kim, Y., and Srinivasan, R. Flow field and wall temperature measurements for reacting flow in a lean premixed swirl stabilized can combustor. *Journal of Engineering for Gas Turbines and Power*, 140(9):091503, 2018. doi: 10.1115/1.4039462.

[13] Albert, J.E., Bogard, D.G., and Cunha, F. Adiabatic and overall effectiveness for a film cooled blade. In *Proceedings of the ASME Turbo Expo*, volume 2, pages 251–259, 2004. doi: 10.1115/GT2004-53998.

[14] Li, M., Li, X., Ren, J., and Jiang, H. Overall cooling effectiveness characteristic and influence mechanism on an endwall with film cooling and impingement. In *Proceedings of the ASME Turbo Expo*, 2015. doi: 10.1115/GT2015-43069.

[15] Nathan, M.L., Dyson, T.E., Bogard, D.G., and Bradshaw, S.D. Adiabatic and overall effectiveness for the showerhead film cooling of a turbine vane. *Journal of Turbomachinery*, 136(3):031005, 2013. doi: 10.1115/1.4024680.

[16] Martiny, M., Schulz, A., and Wittig, S. Mathematical model describing the coupled heat transfer in effusion cooled combustor walls. In *Proceedings of the ASME Turbo Expo*, 1997. doi: 10.1115/97-GT-329.

[17] Shrager, A.C., Thole, K.A., and Mongillo, D. Effects of effusion cooling pattern near the dilution hole for a double-walled combustor liner-part ii: Flowfield measurements. *Journal of Engineering for Gas Turbines and Power*, 141(1):011023, 2019. doi: 10.1115/1.4041153.

[18] Stimpson, C.K., Snyder, J.C., Thole, K.A., and Mongillo, D. Effects of coolant feed direction on additively manufactured film cooling holes. *Journal of Turbomachinery*, 140(11):111001, 2018. doi: 10.1115/1.4041374.

[19] Andreini, A., Facchini, B., Picchi, A., Tarchi, L., and Turrini, F. Experimental and theoretical investigation of thermal effectiveness in multiperforated plates for combustor liner effusion cooling. *Journal of Turbomachinery*, 136(9):091003, 2014. doi: 10.1115/1.4026846.

[20] Charonko, J.J. and Vlachos, P.P. Estimation of uncertainty bounds for individual particle image velocimetry measurements from cross-correlation peak ratio. *Measurement Science and Technology*, 24(6):065301, 2013. doi: 10.1088/0957-0233/24/6/065301.

[21] Martiny, M., Schiele, R., Gritsch, M., Schulz, A., and Wittig, S. In situ calibration for quantitative infrared thermography. In *Proceedings of the 1996 International Conference on Quantitative InfraRed Thermography*. QIRT Council, 1996. doi: 10.21611/qirt.1996.001.

[22] Caciolli, G., Facchini, B., Picchi, A., and Tarchi, L. Comparison between psp and tlc steady state techniques for adiabatic effectiveness measurement on a multiperforated plate. *Experimental Thermal and Fluid Science*, 48:122–133, 2013. doi: 10.1016/j.expthermflusci.2013.02.015.

[23] Sellers, J.P. Gaseous film cooling with multiple ejection stations. *AIAA Journal*, 1(9):2154–2156, 1963. doi: 10.2514/3.2014.